

Quantum-Plasma Model of Atomic Cluster Excitations

A. El-Khawaldeh and H.-J. Kull

Institute for Theory of Statistical Physics, Laser Physics Group, RWTH Aachen University,
52062 Aachen, Germany

E-mail: amir.el@rwth-aachen.de

Abstract. The laser-light absorption of a thin foil is studied in the framework of the self-consistent time-dependent Hartree theory. It is found that asymptotically for large numbers of electron states, a single-state Vlasov model is sufficient to describe the main features of the energy absorption to a very good approximation. Since the single-state model is numerically feasible, this allows one to calculate the energy absorption over a wide range of laser parameters. Studying the size-dependence of the absorption mechanism, quantum-mechanical modifications of the well-known classical Brunel theory can be observed for thin layers.

1. Introduction

This article summarizes parts of the results which were presented at the twenty fifth annual International Laser Physics Workshop (LPHYS'16) in Yerevan, Armenia. In the context of our presentation on the topic 'Quantum-Plasma Model of Atomic Cluster Excitations' we gave an overview on the results we achieved based on quantum-plasma calculations on spherical atomic clusters and thin plasma foils. This paper refers to the results we obtained for thin plasma foils.

The statistical properties of ideal quantum plasmas are commonly described in the framework of the self-consistent quantum Vlasov theory which determines the time evolution of the single-particle density operator. This method corresponds to a quantum-mechanical multi-stream model in which the many-particle system can be described by a finite set of single-particle wave functions interacting via a self-consistent potential [1]. Another effective many-body theory closely related to the Vlasov theory is the time-dependent Hartree theory.

In this work, both models are applied to a thin plasma foil interacting with an external laser field which is considered to be obliquely incident on the foil surfaces. A reduced capacitor model [2] effectively leads to a spatially one-dimensional (1d) description of the electron dynamics. The classical Brunel theory [3] describes the collisionless energy absorption of a plane surface by electrons which are pulled into the vacuum and accelerated in the presence of the laser field. This mechanism dominates the absorption if the solid has a sharp surface and an electron density well above the critical density where the light frequency equals the plasma frequency. In the present work, we focus attention on this non-resonant collisionless absorption. Brunel's theory predicts a characteristic scaling $E_{\text{abs}} \sim \mathcal{E}_0^3$ of the absorbed energy with the electric field amplitude \mathcal{E}_0 of the laser. The absorption mechanism suggested by Brunel has been analyzed classically for thin foils with two surfaces in the framework of a 1d capacitor model [4]. However, if the foil thickness approaches the nanoscale, quantum-size effects of the absorption which have



not been treated so far are expected to become relevant. In this regime, the so-called spill-out effect, which describes the occurrence of a non-vanishing electron density outside the foil, is a non-thermal quantum feature. In this work, we analyze how Brunel's scaling law is affected by quantum effects in thin plasma foils.

2. Multi-Stream Model

In the present model, the background ions are treated in the jellium approximation as a homogeneously charged foil with thickness l and charge density en_0 , where e denotes the elementary charge and $n_{ion} = n_0/Z$ is the density of ions with average charge state Z . The following dimensionless quantities are used for a plasma with plasma frequency $\omega_p = \sqrt{4\pi n_0 e^2 / m_e}$ (CGS units),

$$\begin{aligned} \mathbf{r} &= \sqrt{\frac{m_e \omega_p}{\hbar}} \mathbf{r}^*, & t &= \omega_p t^*, & n &= \frac{n^*}{n_0}, & E &= \frac{E^*}{\hbar \omega_p}, \\ q &= \frac{q^*}{e}, & \varphi &= \varphi^* \left(\frac{\hbar}{m_e \omega_p} \right)^{\frac{1}{2}}, \end{aligned} \quad (1)$$

where \hbar is the reduced Planck constant. Dimensional quantities are denoted by a star. The prefactors in (1) define the units used throughout this work if not otherwise stated. In some figures, we use the length scale $L = \sqrt{\hbar / (m_e \omega_p)}$.

For the description of the electron system, we consider two different approaches. On the one hand, we consider the well-known time-dependent Hartree theory which describes the electron system in terms of N_s single-particle states $\varphi_k(x, t)$ interacting via individual self-consistent potentials $\phi_k(x, t)$,

$$i\partial_t \varphi_k = \left[-\frac{1}{2} \partial_x^2 - \phi_k - \phi_L \right] \varphi_k, \quad (2a)$$

$$\partial_x^2 \phi_k = \frac{1}{N_s} \sum_{k' \neq k} |\varphi_{k'}|^2 - \rho_{ion}, \quad (2b)$$

where ϕ_L corresponds to the external laser potential in the dipole approximation and $\rho_{ion}(x) = \theta(l/2 - |x|)$ is the ionic charge density. The Hartree theory excludes self-interaction in the calculation of the electronic charge density in (2b). It should be noted that in the dimensionless representation (2) the single-particle states are normalized to the length of the foil, $\langle \varphi_k | \varphi_k \rangle = l$. On the other hand, we consider the simple single-state Vlasov model

$$i\partial_t \varphi = \left[-\frac{1}{2} \partial_x^2 - \phi - \phi_L \right] \varphi, \quad (3a)$$

$$\partial_x^2 \phi = |\varphi|^2 - \rho_{ion}, \quad (3b)$$

where the electron system is described by a single electron state $\varphi(x, t)$ interacting with a self-consistent potential $\phi(x, t)$. The single state model (3) corresponds to a reduced version of the quantum Vlasov theory which describes the electron system by a statistical ensemble of N_s single-particle wave functions $\varphi_k(x, t)$ which we call representative electron states [5]. The Vlasov theory reduces to the above single-state model (3) when taking into account only a single representative state, $N_s = 1$. It is noted that the main difference between the Hartree and the Vlasov model arises from the fact that self-energy interaction terms are not included in the Poisson's equations of the Hartree theory.

For the numerical evaluation of the systems (2) respectively (3), a Crank-Nicolson scheme [6] is chosen for the Schrödinger equations in combination with standard finite-difference techniques for Poisson's equation.

3. Results

In this section, we summarize some results obtained for the equilibrium configurations, the single-state Vlasov approximation and finally for the scaling law of the energy absorption.

3.1. Equilibrium States

In the absence of the laser field, $\phi_L = 0$, solutions of the systems (2) and (3) with a time-independent electron density can be written in the form

$$\varphi_k(x, t) = \varphi_k^{(0)}(x)e^{-i\epsilon_k t}. \quad (4)$$

Then, the equilibrium density is given by

$$n^{(0)} = \frac{1}{N_s} \sum_k |\varphi_k^{(0)}|^2. \quad (5)$$

To determine the equilibrium states $\varphi_k^{(0)}$, we choose a relaxation method [7]. Figure 1 shows the equilibrium densities for a foil with thickness $l = 50$. Comparison is made between the single-state model and the Hartree model for different N_s . Furthermore, results for the self-consistent potentials $\phi_k^{(0)}$ in the equilibrium state are shown.

As depicted, the electron density within the Hartree model becomes homogeneous inside the foil as the number of representative states is chosen sufficiently large. The same behavior of the electron density inside the foil can be observed for the single-state Vlasov model.

However, the individual equilibrium states $\varphi_k^{(0)}$ look significantly different from the equilibrium wave function of the single-state Vlasov model. The single-state equilibrium wave function has the same structure as the density. In the case of the Hartree model, each peak of the density is associated with a single-electron equilibrium state k which is localized around the mean position $\langle x \rangle_k$. To get a qualitative interpretation of the equilibrium states and to compare the results to corresponding classical calculations, analytical solutions for the Hartree equilibrium states are calculated asymptotically for $N_s/l \rightarrow 0$. In this limit, the overlap between the electron states is negligible and the equilibrium becomes a set of coherent states of a harmonic oscillator separated by a distance l/N_s ,

$$\varphi_k(x) = \frac{1}{\sqrt[4]{\pi}} e^{-0.5(x-x_k)^2}, \quad x_k = -\frac{l}{2} \left(1 + \frac{1-2k}{N_s} \right), \quad k = 1, 2, \dots, N_s. \quad (6)$$

This result suggests that the Hartree model (2) can be interpreted as the quantum-mechanical analogue of the classical particle model defined in [4]. Thereby, the equation of motion for the point charge k is replaced by the Schrödinger equation for the wave function φ_k . Since the electron density of a single wave function within the Hartree description is not point-like, the calculation of the electrostatic potential is not as simple as for point-particles.

The self-consistent potential of the single-state model exhibits two pronounced minima close to the foil surface which generate the binding of the electrons. The local minima of the potential occur due to the overshoot of the electron density at the foil surface. Within the Hartree model, each electron state sees an individual potential with a single local minimum. As one can see, the potential ϕ_k increases linearly far away from the region electron k is localized to. This fact is related to the 1d nature of the underlying model. According to Poisson's equation in 1d, a localized charge distribution $\rho(x)$ generates a constant electric field $|\mathcal{E}| = |q|/2$ outside the region of its localization. Thus, since a Hartree state sees a charge distribution with total charge $q = l/N_s$, there is no ionization in the present Hartree model and an outgoing electron will always be accelerated back to the foil. This feature of the 1d description is not present in

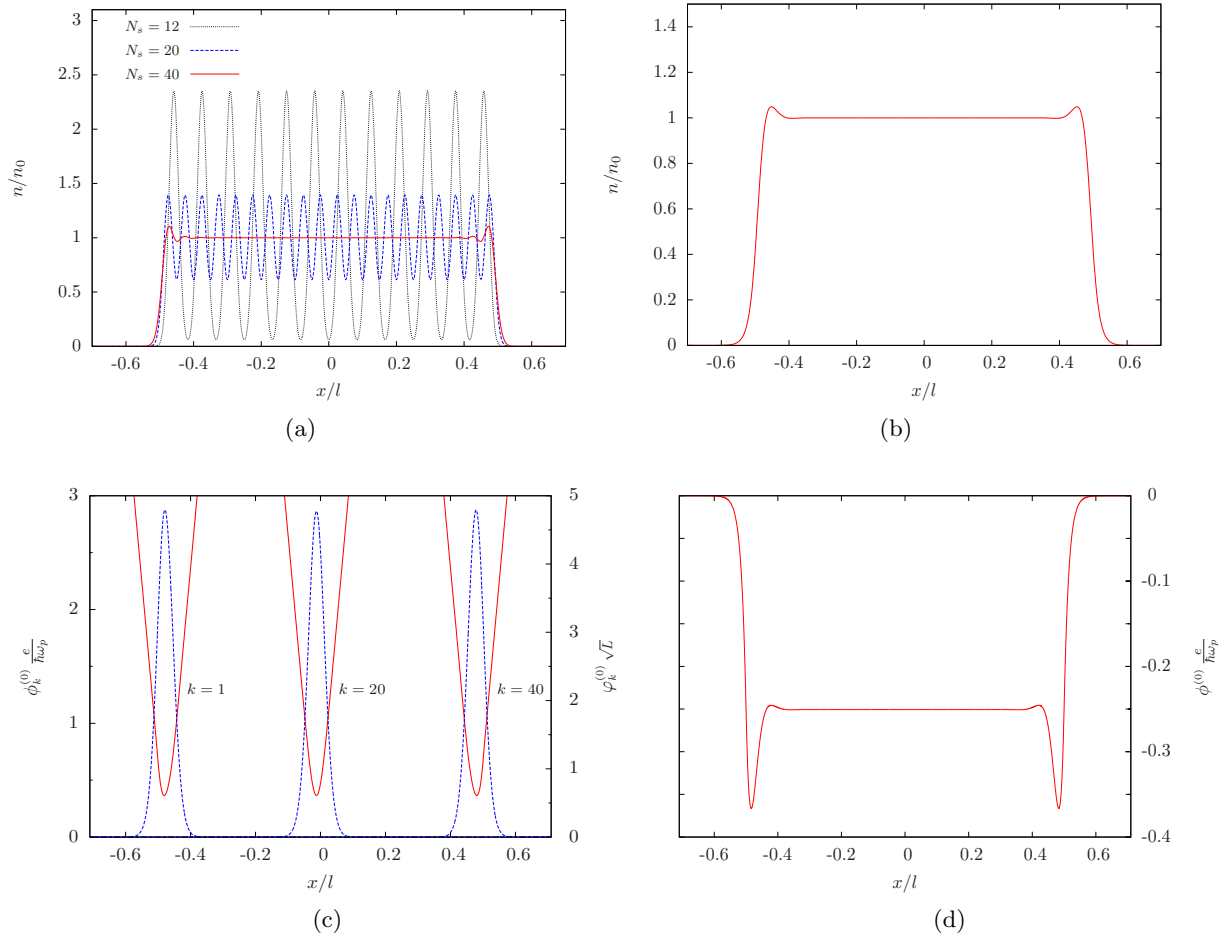


Figure 1. Equilibrium quantities for a foil with thickness $l = 50$. The figure shows the equilibrium densities for (a) the Hartree and (b) the single-state model. Furthermore, exemplary results for the self-consistent potentials in the equilibrium state are shown for (c) the Hartree model with $N_s = 40$ and (d) the single-state model. In the case of the Hartree model, the corresponding equilibrium wave functions $\varphi_k^{(0)}$ are indicated.

the single-state model since the self-consistent potential is calculated from a neutrally charged distribution.

Furthermore, figures 1a and 1b clearly show the spill-out effect of the electron density at the foil surface. To investigate the regime of l -values for which quantum effects are suggested to become significant, we analyze how the spill-out effect depends on the size of the foil. Figure 2 shows the fraction of spill-out electrons f_{out} as a function of the foil thickness in the single-state model. One calculates for $l = 5$ that 13% of the electrons are located outside the foil in the equilibrium state. For $l \gtrsim 5$, it is found that f_{out} scales with the inverse foil thickness. A fit to the data with $l \gtrsim 5$ using the model function $f_{out}(l) = \alpha/l^\beta$ yields the values $\alpha = 0.659$ and $\beta = 0.997$. In the following, the plasma foil is exposed to a laser field. Before the interaction with the laser at $t = 0$, the electron system is considered to be in the equilibrium state.

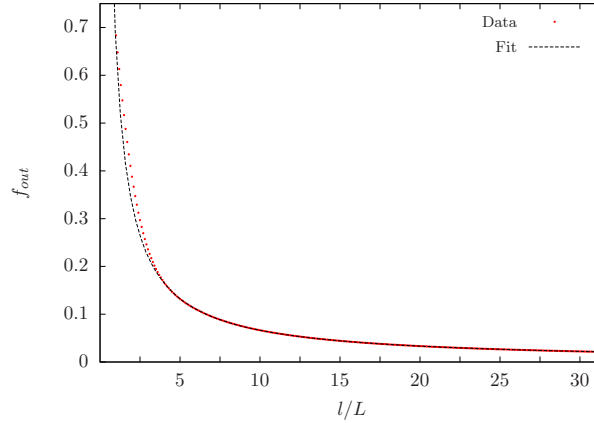


Figure 2. Fraction of spill-out electrons as a function of the foil thickness. The data points are fitted to the inverse power law $f_{out} = 0.659/l^{0.997}$.

3.2. Comparison of Hartree Model and Single-State Model

The numerical calculation of the electron dynamics in the presence of strong laser fields based on the Hartree model (2) requires on the one hand large spatial grids to account for fast electrons moving far away from the foil and on the other hand small numerical grid constants with respect to the time variable to resolve their dynamics. These requirements are already present in classical PIC calculations. Since the present quantum-mechanical description furthermore requires small spatial grid constants to resolve small de Broglie wavelengths, calculations with large N_s become time-consuming. Since we are interested in macroscopic quantities like the absorbed energy per electron, it is an instructive task to analyze two major questions. Does the dynamics of the electron system converge if the number of electron states N_s is chosen sufficiently large? If yes, is the single-state Vlasov model capable of describing the main features of the energy absorption? In particular, the last point is of great interest since calculations within the single-state Vlasov model are numerically feasible which allows one to perform calculations over a wide range of laser parameters. In order to investigate the above questions, we performed test calculations within the Hartree model for different N_s and the single-state model in the presence of a strong laser field compared to the electric field generated by the ions.

In the following, the laser field is considered in the electric dipole approximation. A \sin^2 -pulse with n laser cycles, frequency ω and pulse duration $\tau = 2\pi n/\omega$ is chosen for the electric field of the laser,

$$\phi_L(x, t) = -x\mathcal{E}(t), \quad \mathcal{E}(t) = \mathcal{E}_0 \sin(\pi t/\tau)^2 \sin(\omega t). \quad (7)$$

The mean total energy of the foil per electron is calculated based on the expectation values of the single-particle energies,

$$\frac{E_{tot}}{N_e} = \frac{1}{N_s} \sum_{k=1}^{N_s} \frac{\langle \varphi_k | E_k | \varphi_k \rangle}{\langle \varphi_k | \varphi_k \rangle} + \frac{E_{ion}}{N_e}, \quad (8)$$

$$E_k = T + V_k, \quad T = -\frac{1}{2} \frac{\partial^2}{\partial x^2}, \quad V_k = -\phi^{(ion)} - \frac{1}{2} \phi_k^{(e)}. \quad (9)$$

where E_{ion} is the potential energy of the ion system in its own field which is a constant value within the jellium approximation. The operator T corresponds to the kinetic energy operator. The potentials $\phi^{(ion)}$ and $\phi_k^{(e)}$ specify the ion and the electron contribution to the self-consistent potential in (2b) respectively (3b), $\phi_k = \phi^{(ion)} + \phi_k^{(e)}$. It is noted that the single-particle energy

operator E_k does not coincide with the single-particle Hamiltonian in the present self-consistent description. The prefactor $1/2$ in the definition of the potential energy V_k has to be taken into account in order to avoid double-counting of the electron-electron interaction energy.

For the test calculation, a foil with $l = 10$ is considered. Since we want to perform the calculations over a wide range of N_s -values, we choose a sufficiently short single-cycle pulse ($n = 1$) with $\omega = 0.125$ and $\mathcal{E}_0/\mathcal{E}_{ion} = 40\%$ in order to make the calculation numerically affordable. Here, $\mathcal{E}_{ion} = l/2$ corresponds to the maximal value of the ionic field which is achieved at the foil boundary. Figure 3 shows the dynamics of the center of mass (COM)

$$X(t) = \frac{1}{N_s} \sum_{k=1}^{N_s} \frac{\langle \varphi_k | \hat{x} | \varphi_k \rangle}{\langle \varphi_k | \varphi_k \rangle} \quad (10)$$

as a function of time as well as the absorbed energy $E_{abs} = E_{tot}(\tau) - E_{tot}(0)$ per electron for different N_s . For the considered value of \mathcal{E}_0 , the grid constants have to be chosen quite small, $\Delta x \lesssim 0.01$ and $\Delta t \lesssim 0.001$, in order to observe convergence of the numerical solution. To avoid boundary effects driven by outgoing electrons, one has to choose a spatial grid with about 10^5 grid points.

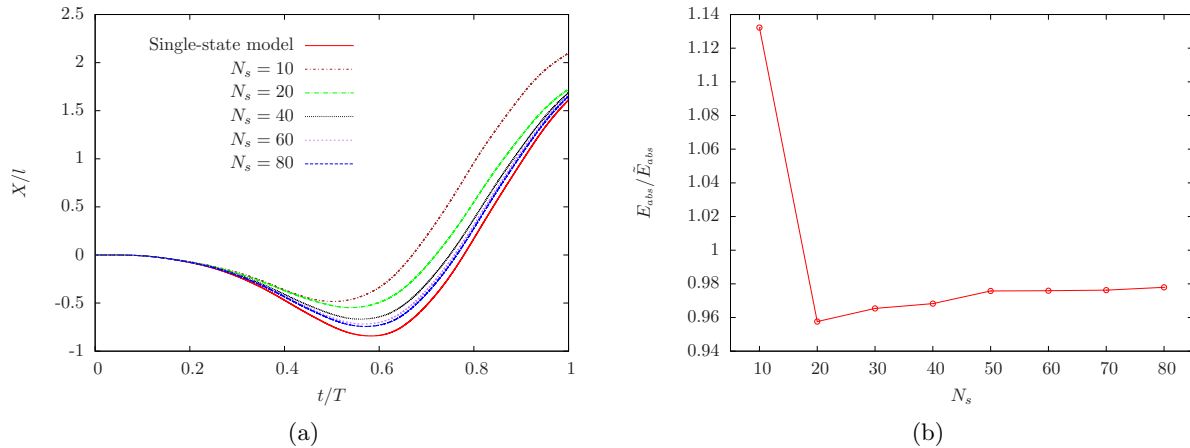


Figure 3. Motion of (a) the center of mass and (b) the absorbed energy per electron for a laser pulse with $n = 1$, $\omega = 0.125$ and $\mathcal{E}_0/\mathcal{E}_{ion} = 40\%$. The results are shown for different numbers of electron states N_s within the Hartree model and the single-state Vlasov model. In (b), the absorbed energy is measured in units of the energy \tilde{E}_{abs} absorbed within the single-state Vlasov model.

Figure 3a shows that the electrons are pulled in the negative direction within the first half of the laser cycle. Thereby, a large number of electrons leave the foil. Within the second half of the cycle, electrons are accelerated back and gain enough energy to move through the foil. A large displacement of the electron system with respect to the equilibrium state can be observed at the end of the pulse.

As depicted in Figure 3b, the absorbed energy deviates from the single-state result by more than 10% for the smallest considered value of $N_s = 10$. As shown in Figure 1, also the corresponding equilibrium density looks pretty different from the single-state result. However, for $N_s > 10$ one can see that the deviation of the absorbed energy is less than 5% and varies only slightly over the range of considered N_s -values. For the largest considered value of $N_s = 80$, the Hartree result differs from the single-state result by an amount of approximately 2%. This result suggests that the single-state model is able to reproduce the absorption of the many-particle system to a good approximation if the number N_s is chosen sufficiently large.

3.3. Energy Absorption as a Function of the Laser Field Strength

In this section, we analyze the energy absorption of the foil as a function of the field strength of the laser. Brunel described the electron dynamics at a single sharp surface by an ensemble of single-particle trajectories interacting via an electrostatic potential [3]. As a major result, it was found that the absorbed energy of the surface per electron can be written in the form

$$\frac{E_{abs}}{N_e} = \frac{1}{2} \eta \frac{\mathcal{E}_0^3}{\omega^2} \frac{1}{l}, \quad (11)$$

where η is a numerical constant which depends on the pulse duration. It should be noted that the result of Brunel is given in (11) in terms of the plasma units (1), where the length dependence is due to these units. The absorption mechanism of vacuum heating for a foil with two sharp surfaces has been analyzed classically [4]. It was found that the absorbed energy can be represented by a scaling law similar to (11) but with a different numerical value for η . From a classical point of view, the characteristic scaling of the absorbed energy with the third power of \mathcal{E}_0 in the non-resonant case can be motivated based on the assumption that the energy absorption is mainly driven by electrons which leave the foil. Since our quantum results will be compared to the classical results of Brunel, we shortly summarize the main points. For the estimation of the absorbed energy, we approximate the COM-motion by the equation of motion without surface effects,

$$\ddot{X} + X = -\mathcal{E}(t). \quad (12)$$

In the non-resonant limit $\omega \ll 1$, the solution reads $X(t) = -\mathcal{E}(t)$ with a maximal displacement of $X_0 = \mathcal{E}_0$. Since the equilibrium density is spatially homogeneous in the classical description, the maximum number N_{out} of electrons which leave the foil over one laser cycle is given by

$$N_{out} = n_0 X_0^* = \frac{N_e}{l} \mathcal{E}_0. \quad (13)$$

Electrons which are pulled into the vacuum are accelerated by the laser field and gain an amount of energy proportional to the mean quiver energy $U_p \sim \mathcal{E}_0^2$ of a free electron in a laser field, known as the ponderomotive potential. With this consideration, the absorbed energy exhibits a scaling of the form $E_{abs} \sim \mathcal{E}_0^3$.

In the following, we analyze the energy absorption of the foil as a function of the laser field strength. Due to the fact that the cycle-averaged absorbed energy is not expected to vary significantly during the main part of a few-cycle pulse [4], we choose for simplicity a single-cycle pulse and an overdense foil with $\omega = 0.1$. Figure 4 shows the absorbed energy per electron as a function of \mathcal{E}_0 for two foils with $l = 5$ and $l = 50$. On the double-logarithmic scale, one can clearly identify two regimes of \mathcal{E}_0 -values for $l = 5$ which can be represented by scaling laws $E_{abs}/N = \alpha \mathcal{E}_0^\beta$. A fit yields the values $\alpha = 5.65$, $\beta = 3.33$ for $\mathcal{E}_0/\mathcal{E}_{ion} \lesssim 0.2$ and $\alpha = 5.13$, $\beta = 2.98$ for $\mathcal{E}_0/\mathcal{E}_{ion} \gtrsim 0.4$. The two fits are also indicated in Figure 4. Two scaling regimes can also be found for the thicker foil with $l = 50$. A fit yields the values $\alpha = 0.43$, $\beta = 3.15$ for $\mathcal{E}_0/\mathcal{E}_{ion} \lesssim 0.02$ and $\alpha = 0.4$, $\beta = 3.07$ for $\mathcal{E}_0/\mathcal{E}_{ion} \gtrsim 0.04$.

In summary, for sufficiently large values of \mathcal{E}_0 , one can observe a scaling which is pretty close to the one predicted within Brunel's theory with a scaling exponent close to 3. However, for the smaller foil one can clearly see a deviation from the classical behavior over a wide range of \mathcal{E}_0 -values. Since this effect is less pronounced for the large foil, we conclude that the deviation can be referred to quantum-size effects which become relevant for small foils. To investigate how the increased scaling exponent of E_{abs}/N_e emerges for small foils, we compare the scaling of the maximum number of free electrons (13) in Brunel's theory to a corresponding value within the present quantum-mechanical treatment. As a measure for the fraction of free electrons, we

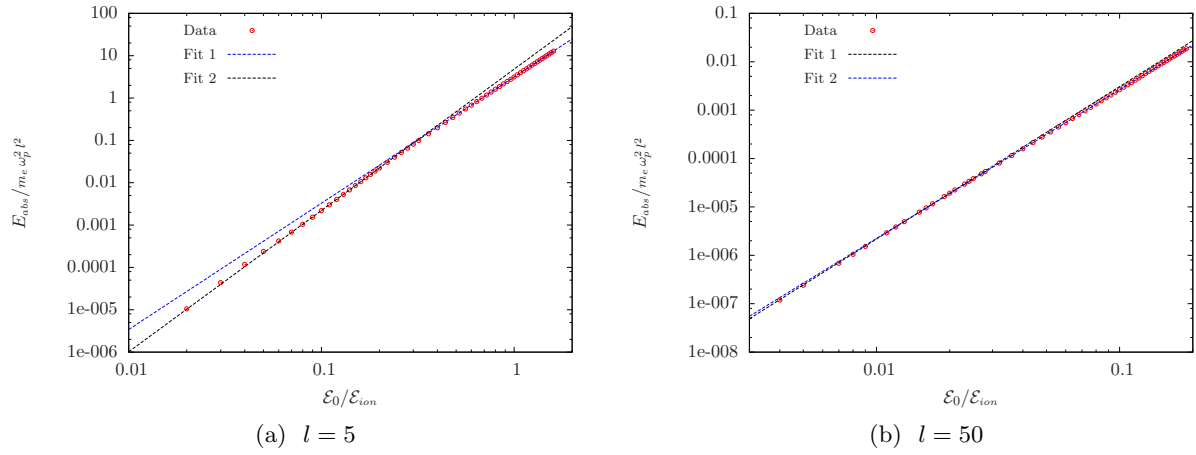


Figure 4. Absorbed energy per electron as a function of the laser field strength \mathcal{E}_0 for two foils with thickness $l = 5$ and $l = 50$. A laser pulse with $n = 1$ and $\omega = 0.125$ is chosen. The results are shown for different field strengths \mathcal{E}_0 measured with respect to the maximal value of the ionic field \mathcal{E}_{ion} . The data points are fitted to model functions of the form $E_{abs}/N = \alpha \mathcal{E}_0^\beta$.

calculate the time-averaged fraction of electrons \bar{f}_{out} which are located outside the foil during the laser-foil interaction,

$$\bar{f}_{out} = \frac{1}{\tau} \int_0^\tau f_{out}(t) dt, \quad f_{out}(t) = 1 - \frac{1}{N_e} \int_{-\frac{L}{2}}^{\frac{L}{2}} n(x, t) dx. \quad (14)$$

Figure (5) shows the results for the two foils with thickness $l = 5$ and $l = 50$. One clearly

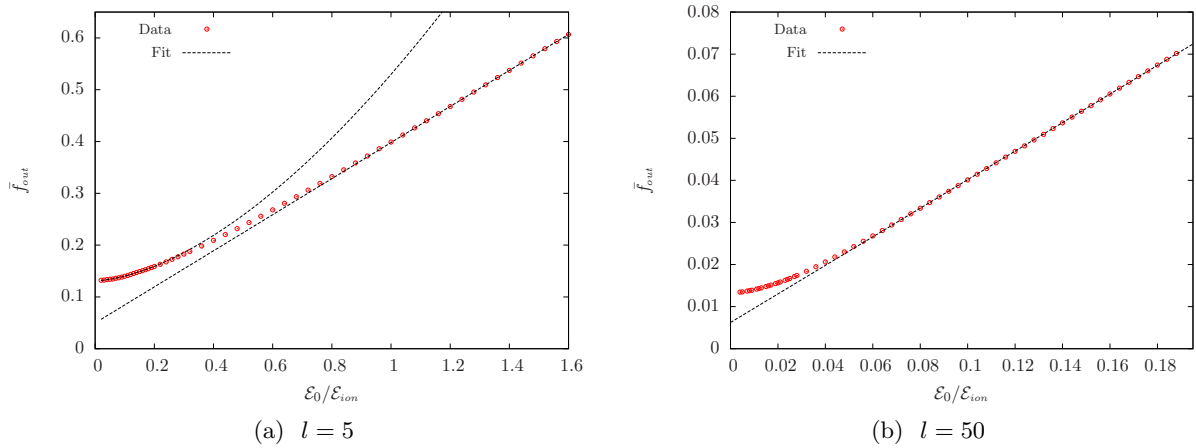


Figure 5. Time-averaged fraction of electrons which are located outside the foil during the interaction with the laser ($\omega = 0.125, n = 1$). The results are shown for different laser field strengths \mathcal{E}_0 measured with respect to the maximal value of the ionic field \mathcal{E}_{ion} . The data points for strong laser fields are fitted to a linear function.

identifies a linear dependence of \bar{f}_{out} on \mathcal{E}_0 for sufficiently high values of \mathcal{E}_0 . Thereby, one recognizes that the linear dependence is already fulfilled for $\mathcal{E}_0/\mathcal{E}_{ion} \gtrsim 0.06$ in the case of the large

foil with $l = 50$, while it requires much stronger fields $\mathcal{E}_0/\mathcal{E}_{ion} \gtrsim 1$ compared to the ionic field to observe a linear dependence in the case of the small foil with $l = 5$. To investigate the increase of \bar{f}_{out} in the regime of \mathcal{E}_0 -values for which a faster increase of the absorbed energy can be observed, a fit is performed to the data with $\mathcal{E}_0/\mathcal{E}_{ion} \lesssim 0.2$ using the model function $\bar{f}_{out}(\mathcal{E}_0) = \alpha \mathcal{E}_0^\beta + \gamma$. The fit yields the values $\alpha = 0.088$, $\beta = 1.65$, $\gamma = 0.13$ and is also indicated in Figure 5a. Here, γ corresponds to the fraction of spill-out electrons in the equilibrium state. The result indicates that \bar{f}_{out} grows faster as a function of \mathcal{E}_0 for small fields, where a faster increase of the absorbed energy can be observed compared to the Brunel-like behavior for $\mathcal{E}_0/\mathcal{E}_{ion} \gtrsim 1$.

The different behavior of \bar{f}_{out} for thin foils can be understood in terms of the surface profiles of the equilibrium density. Decreasing the foil thickness, the transition region of the equilibrium density shown in Figure 1b is broadened. We consider a shift of the equilibrium distribution by an amount ξ along the x -axis, where $N_{out}(\xi)$ is the number of electrons which leave the foil due to the displacement. In the classical case, one has $N_{out} \sim \xi$ due to the homogeneity of the equilibrium density inside the foil. If the electron density is broadened, the expansion of $N_{out}(\xi)$ with respect to ξ also contains higher orders of ξ . However, if the deflection is chosen sufficiently large such that the inhomogeneous part of the equilibrium density is already located outside the foil, the density distribution becomes homogeneous at the foil boundary and a further increase $d\xi$ generates a number of outgoing electrons $dN_{out} \sim d\xi$.

The scaling law

$$\frac{E_{abs}}{N_e} = a(l) \mathcal{E}_0^b \quad (15)$$

we found for large values of \mathcal{E}_0 , with values of b close to 3 and a constant a which depends on the foil thickness, allows for a comparison with the corresponding classical result calculated in [4]. The authors find a scaling law similar to the result (11) of Brunel with a numerical constant of $\eta = 8.75$ for a laser pulse with $n = 10$ laser cycles. The corresponding value for a single-cycle pulse is given by $\eta = 0.875$, where we divided the result $\eta = 8.75$ suggested in [4] by the number of laser cycles. For the comparison with our results, we evaluate the a -parameter of the classical result (11) with the laser frequency $\omega = 0.125$ we used in our calculations,

$$a = \frac{0.875}{2} \frac{1}{0.125^2} \frac{1}{l} = \frac{28}{l}. \quad (16)$$

We calculate the a -parameter based on our calculations for different values of l . The results are shown in Figure 6. A model function $a(l) = \alpha/l^\beta$ is fitted to the data which is also presented in Figure 6. We obtain the fit parameters $\alpha = 30.1$ and $b = 1.09$. One can see that the found value of α is close to the value 28 suggested by the classical result (16).

4. Conclusion

In the presented work, we have analyzed the energy absorption of a thin foil based on the Hartree model and a single-state Vlasov model. We found that the energy absorption within the Hartree model can be described to a very good approximation by the simple Vlasov model if the number of electron states is chosen sufficiently large. For a foil with thickness $l = 10$ and $N_s = 80$ electron states, we have found that the Hartree and the single-state result for the absorbed energy differ only by 2%.

At sufficiently high laser fields, we found that the energy absorption can be represented by a simple scaling law $E_{abs} \sim \mathcal{E}_0^b$, where the numerical value of b is close to the value 3 predicted by the classical Brunel theory independent of the foil thickness. For thin foils where quantum-size effects are relevant, we found that the scaling exponent is larger than the value $b = 3$ over a wide range of laser field strengths.

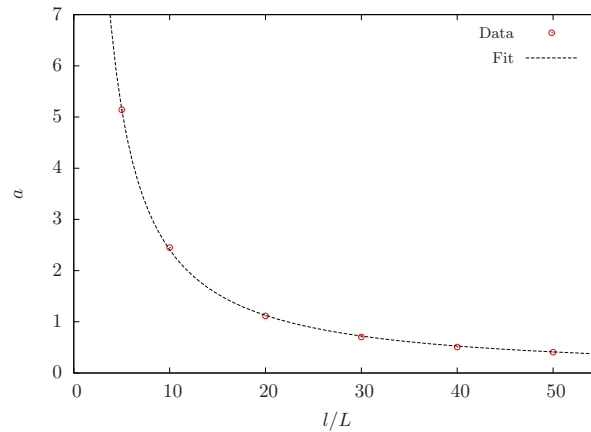


Figure 6. Scaling parameter a as a function of the layer thickness l . The data points are fitted to the inverse power law $a = 30.1/l^{1.09}$.

References

- [1] Haas F, Manfredi G and Feix M 2000 *Phys. Rev. E* **62**(2) 2763–2772
- [2] Forslund D W, Kindel J M, Lee K and Lindman E L 1976 *Phys. Rev. Lett.* **36**(1) 35–38
- [3] Brunel F 1987 *Phys. Rev. Lett.* **59**(1) 52–55
- [4] Greschik F, Dimou L and Kull H J 2000 *Laser and Particle Beams* **18** 367–373
- [5] Schmidt-Bleker A, Gassen W and Kull H J 2011 *EPL (Europhysics Letters)* **95** 55003
- [6] Crank J and Nicolson P 1947 *Mathematical Proceedings of the Cambridge Philosophical Society* **43**(01) 50–67
- [7] Goldberg A and Schwartz J L 1967 *Journal of Computational Physics* **1** 433 – 447